Transport mechanism in polycrystalline $La_{0.825}Sr_{0.175}Mn_{1-x}Cu_xO_3$

Li Pi, Lei Zheng, and Yuheng Zhang
Structure Research Laboratory, University of Science and Technology of China, Academia Sinica, Hefei 230 026, People's Republic of China
(Received 10 August 1999)

The transport mechanism of polycrystalline samples $La_{0.825}Sr_{0.175}Mn_{1-x}Cu_xO_3$ ($0 \leqslant x \leqslant 0.20$) and the effects of Cu doping have been investigated. It can be concluded that the existence of Cu induces the superexchange interaction and weakens the long range ferromagnetic order in the samples. The transport mechanism in the metallic regime is attributed to the magnon-carrier scattering and the transport mechanism in the insulating regime transits from polaron transport to variable-range hopping with the adding of Cu. The effect of the surface phase is also observed in the samples.

I. INTRODUCTION

Recently, doped manganese perovskites have attracted much renewed attention due to the discovery of colossal magnetoresistance (CMR).[1–3] In the systems of $Ln_{1-x}A_xMnO_3$ (Ln=La-Tb, and A=Ca, Sr, Ba, Pb, etc.), the existence of the dopant leads to mixed valency of the Mn ions (Mn^{3+}/Mn^{4+}). In proper content the mixed valency can result in strong ferromagnetic (FM) interactions which can be explained by the double-exchange mechanism (DE).[4] In addition to DE interactions the strong coupling of the vibrational and electronic system in the $Ln_{1-x}A_xMnO_3$ lattice was found to play an important role in the mechanism of the CMR.[5,6] In particular, the Jahn-Teller (JT) effect was believed to affect both the magnetic and transport properties of the $Ln_{1-x}A_xMnO_3$ system.[6,7] In order to get further understanding of the mechanism. Mn site doping effect has been studied.[8–13] A. Barnabé *et al.*[8] found that the substitution of Mn by Cr suppresses the charge ordering and induces ferromagnetism. The research work by Gayathri *et al.*[9] suggests that Co substitution for Mn dilutes the DE mechanism and changes the long range FM order of $La_{0.7}Ca_{0.3}MnO_3$ to a cluster glass-type FM order. However, this kind of research is quite inadequate. We consider that in the CuO plane of high-temperature superconductors, the hybridization between the $3d$ electrons of Cu and the $2p$ electrons of O leads to a strong antiferromagnetic coupling. Because the radius of Cu^{2+} ion is close to that of Mn^{3+} ion, the Mn site can be occupied by Cu. So if Cu is doped into manganese oxide, useful information for understanding the transport mechanism of CMR oxides could be obtained. In this paper, the $La_{0.825}Sr_{0.175}Mn_{1-x}Cu_xO_3$ ($0 \leqslant x \leqslant 0.20$) has been studied. It is found that the bivalent Cu^{2+} cations induce the antiferromagnetic superexchange interaction and destroy the double exchange interaction in the samples. The transport mechanism transits from the polaron transport to variable-range hopping with the increase of Cu^{2+} ions. The effect of the surface phase has also been discussed.

II. EXPERIMENT

The samples were prepared by the usual solid-state reaction method with specpure La_2O_3, $SrCO_3$, MnO_2, and CuO as the starting materials. The mixture of these starting materials were heated in air at 1300 °C for 24 h. Then the powder was ground, palletized, and sintered at 1350 °C for another 24 h. Finally, the furnace was cooled down to room temperature. To the as-obtained samples, we have carried out the

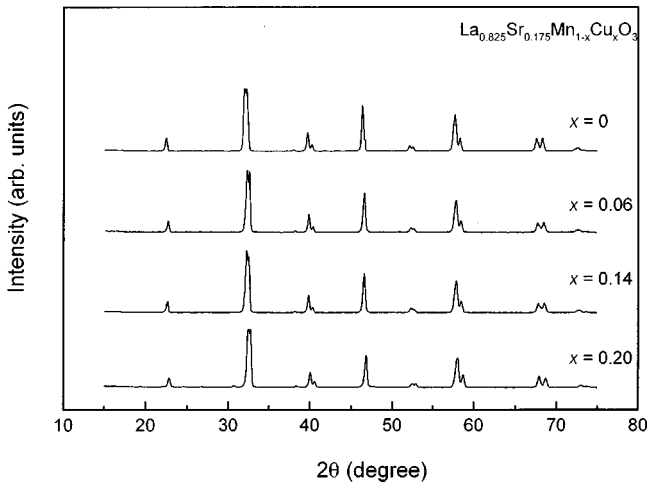

FIG. 1. The XRD patterns of $La_{0.825}Sr_{0.175}Mn_{1-x}Cu_xO_3$.

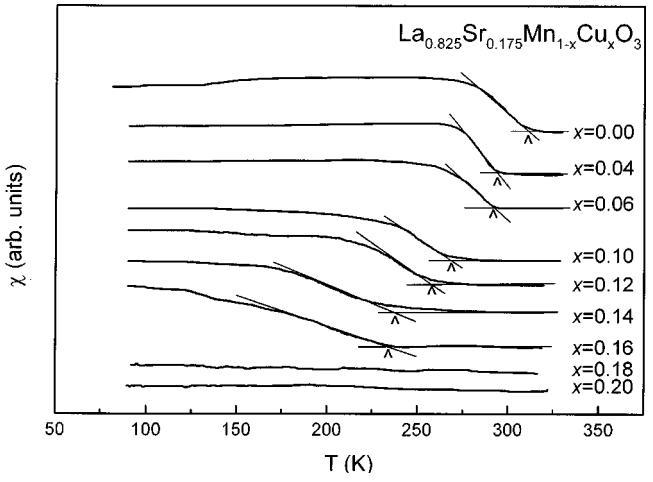

FIG. 2. The susceptibility versus temperature curves of $La_{0.825}Sr_{0.175}Mn_{1-x}Cu_xO_3$. The position marked with ^ represents the T_C^{onset}.

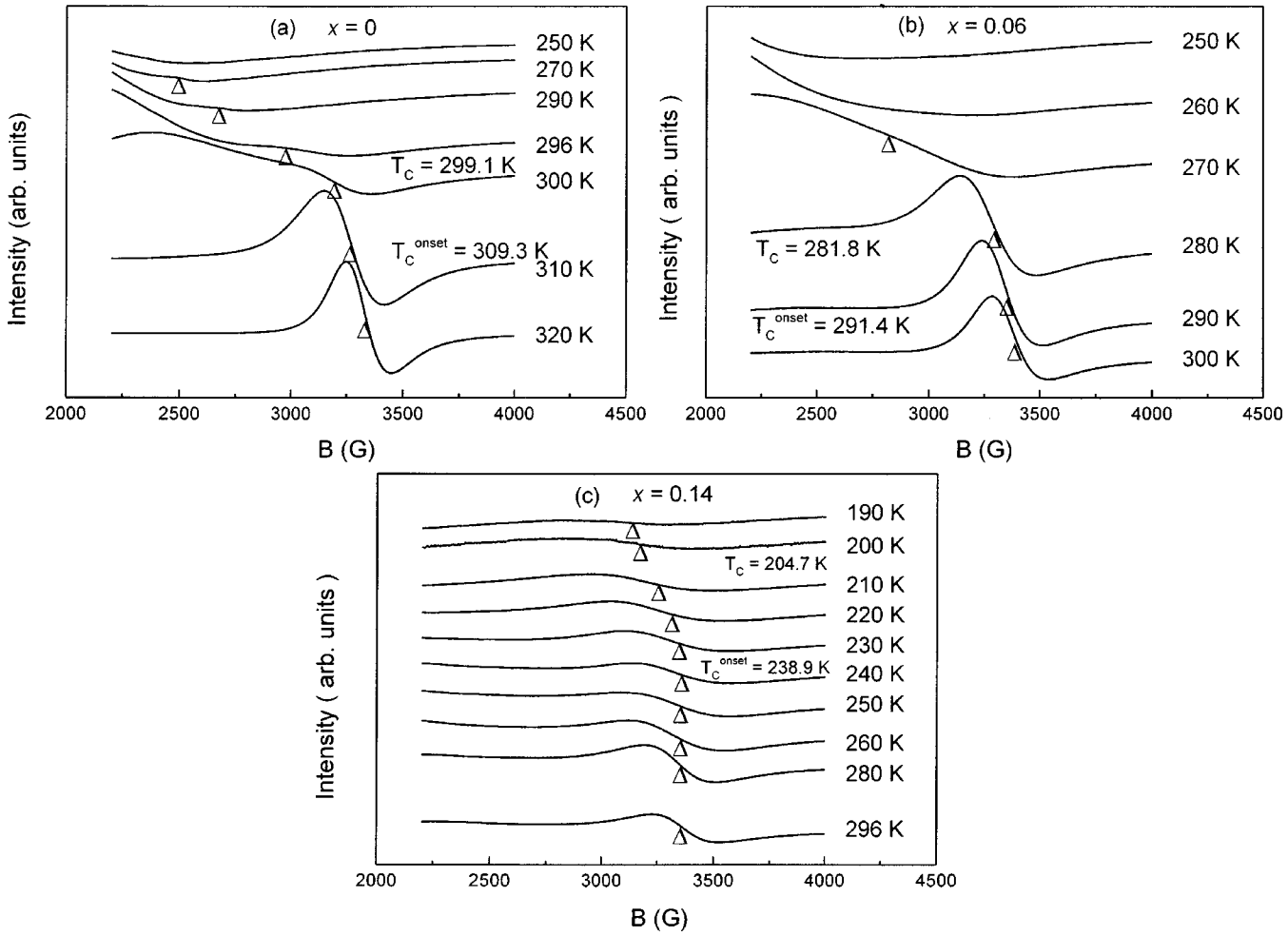

FIG. 3. The changes of ESR signal with temperature. (a) $x=0$; (b) $x=0.06$; (c) $x=0.14$. The peaks marked with Δ are paramagnetic peaks.

following measurements: the x-ray diffraction, ac magnetic susceptibility (χ), electron spin resonance (ESR), resistivity (ρ), and magnetoresistance (MR).

The x-ray diffraction patterns (shown in Fig. 1) were obtained from Japan Rigaku D/max-γa rotating powder diffractometer using Cu K_α radiation. The detective range is 15° to 75°. It indicates that up to $x=0.20$ the samples are single phase. On substitution of Mn by Cu, no structure change has been observed.

ac susceptibility measurements have been carried out in the temperature range 80–325 K, at a magnetic field amplitude of 0.5 Gs and a frequency of 108 Hz. The ESR signals were measured using a BRUKER ER-200D spectrometer at 9.46 GHz. The resistivity under zero and 5 T magnetic field was measured by the standard four-probe method in the temperature range from 20 to 325 K.

III. RESULTS AND DISCUSSION

A. Magnetic properties

Figure 2 shows the ac susceptibility versus temperature curves. In the doping level $0\leqslant x\leqslant 0.16$, all samples display a paramagnetic (PM) to FM phase transition. The Curie tem-

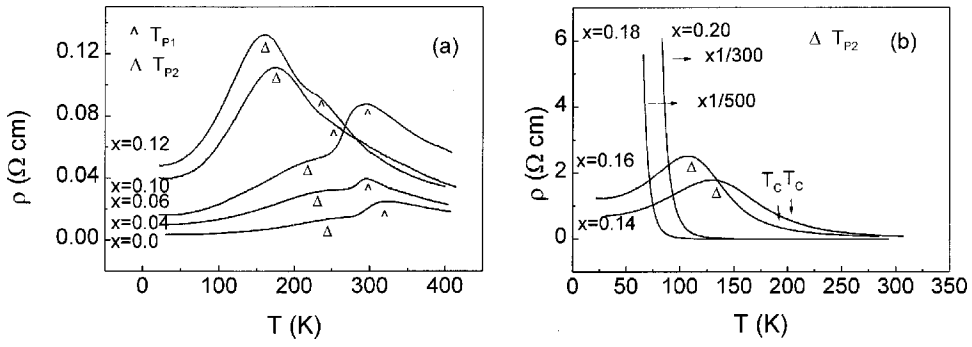

FIG. 4. The resistivity versus temperature curves of $La_{0.825}Sr_{0.175}Mn_{1-x}Cu_xO_3$. (a) $0\leqslant x\leqslant 0.12$; (b) $0.14\leqslant x\leqslant 0.20$.

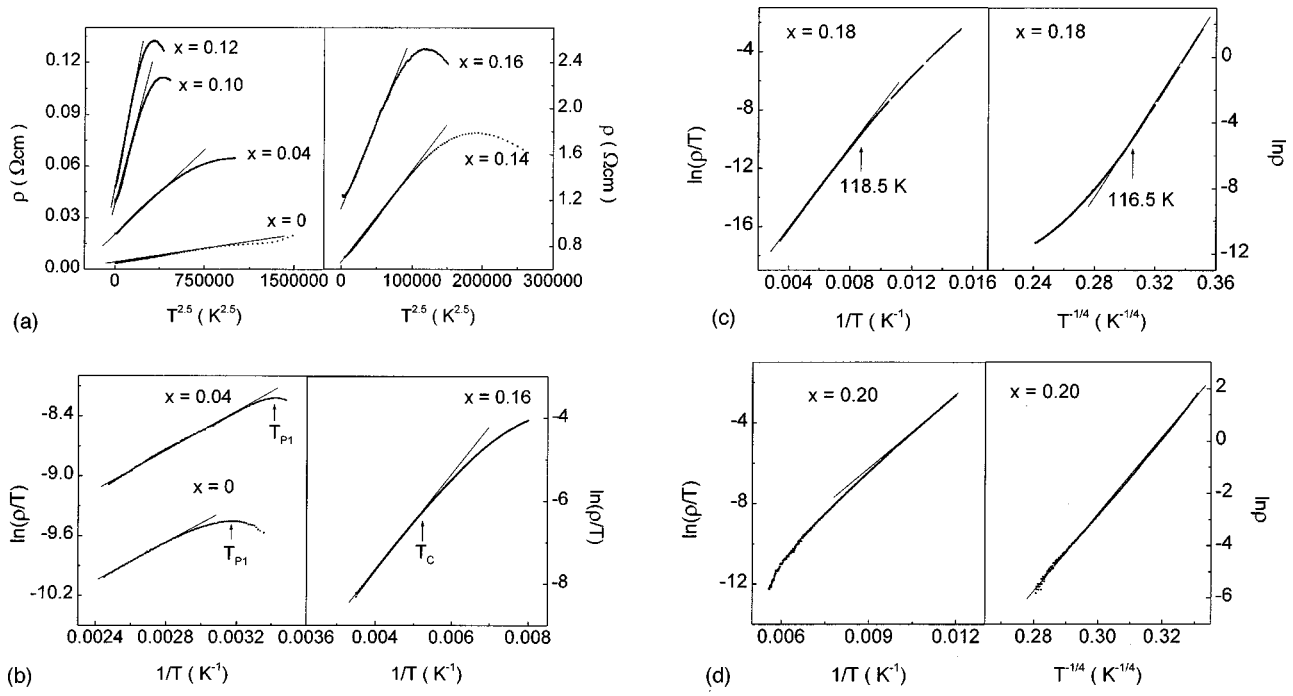

FIG. 5. The fitting of resistivity curves of $La_{0.825}Sr_{0.175}Mn_{1-x}Cu_xO_3$. The dotted lines represent the experimental data. (a) The $\rho \sim T^{2.5}$ curves of low temperature zones. (b) The $\ln(\rho/T) \sim 1/T$ curves for the samples with $x=0$, 0.04, and 0.16. [(c),(d)] The $\ln(\rho/T) \sim 1/T$ curves as well as $\ln \rho \sim T^{-1/4}$ curves for the samples with $x=0.18$ and $x=0.20$.

perature T_C, which is defined as the peak temperature of the differential curves of $\chi \sim T$, decreases from 299.1 K to 190.5 K and T_C^{onset} drops from 309.3 K to 233.4 K with the increase of x. Here T_C^{onset} is the onset temperature of PM-FM phase transition which is determined by the crossing point of the extension line of PM regime and the tangent line of phase transition regime (i.e., the regime with the largest $d\chi/dT$). It is marked with ˆ in Fig. 2. Meanwhile, the magnetism is weakened and the range of the magnetic transition is broadened. When $x \geqslant 0.18$ the samples have no obvious magnetic transition. So it can be concluded that the ferromagnetism of the samples decreases with the increase of Cu. It suggests that although the Cu^{2+} substitution enhances the content of the Mn^{4+} ions, this effect is less considerable for transport process. With the adding of Cu, an antiferromagnetic superexchange interaction is induced and increased.[13–16] At the same time, the Mn^{3+}-O^{2-}-Mn^{4+} bonds are destroyed gradually. This causes the e_g electrons of Mn^{3+} ions localized. So the double exchange interaction in the samples is weakened by the increase of Cu, which caused that the electron spins form the FM alignment at lower temperature. Therefore, the temperature of PM-FM phase transition decreases and the transition range is broadened. In the heavily doped range, the existence of Cu causes a magnetic disorder. Therefore the double exchange interaction is hard to form and the magnetic transition cannot occur.

The ESR properties for $La_{0.825}Sr_{0.175}MnO_3$ are consistent with the experimental results reported by other groups.[17–19] Figures 3(a)–3(c) show the temperature dependence of ESR signal for the samples with $x=0$, 0.06, and 0.14, respectively. It can be seen from Fig. 3(a) that there are clear PM lines with g factor near 2 (marked with Δ) above 300 K. So the sample is in PM phase. Below 300 K, the PM line shifts to low magnetic field and decreases gradually with cooling. It suggests that the sample undergoes a PM-FM phase transition around 300 K. Because the FM regime appears at the phase transition temperature, the remained PM regime is actually surrounded by an internal magnetic field induced by the FM phase. Therefore at a lower applied magnetic field, the sum of the internal and applied field can reach the needed magnitude of the resonance field. So the PM line is located at a lower field. With the decrease of temperature, the FM phase becomes dominant and the PM phase vanishes gradually. Hence, the PM line of ESR decreases and disappears at last. It is similar for the other two samples. For the sample with $x=0.06$, the magnetic transition temperature is around

TABLE I. The Curie temperature T_C and transition temperature T_P for the samples with different x.

x	0	0.04	0.06	0.10	0.12	0.14	0.16	0.18	0.20
T_C(K)	299.1	286.9	281.8	250.2	238.5	204.7	190.5		
T_C^{onset}(K)	309.3	293.7	291.4	269.9	259.0	238.9	233.4		
T_{P1}(K)	313.2	295.5	291.2	245.2	230.1				
T_{P2}(K)	258.5	241.7	230.2	174.6	160.5	129.1	106.6		

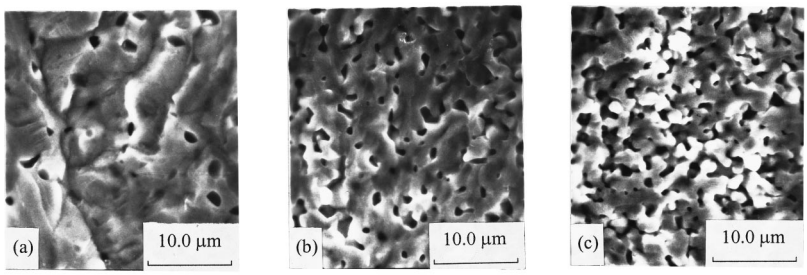

FIG. 6. The scanning electronic microscope photo of $La_{0.825}Sr_{0.175}Mn_{1-x}Cu_xO_3$. (a) $x=0$; (b) $x=0.08$; (c) $x=0.12$.

280 K. And for the sample with $x=0.14$, the transition temperature is between 200 K and 240 K. These results demonstrate through microscopic view that the PM-FM transition actually occurs in the samples. And the transition temperatures determined from ESR are consistent with that of the susceptibility measurements. Furthermore, the existence of the PM lines demonstrates that there actually exists the environment for the formation of magnetic polarons above T_C. With the doping of Cu, this environment is destroyed gradually, which can be seen in the transport measurement.

B. Transport properties

The resistivity versus temperature curves are shown in Fig. 4. It can be seen that in the range $0 \leqslant x \leqslant 0.16$ there is an insulator-metal transition while for the sample with $x \geqslant 0.18$ the transition is not observed. At the same time, the resistivity increases dramatically with the adding of Cu.

In order to investigate further, we have fitted the $\rho \sim T$ curves of Fig. 4. We used $\rho=\rho_0+AT^{2.5}$ to fit the metallic regime. Figure 5(a) shows that the $\rho \sim T^{2.5}$ curves of this regime are nearly linear. It suggests that the transport mechanism of this regime can be attributed to the magnon-carrier scattering, which demonstrates further that the metallic regime is actually in FM phase. To the insulating regime, we have fitted the curves of the samples with $x=0$, 0.04, 0.16, 0.18, and 0.20. For the samples with $x=0$, 0.04, and 0.16, we replotted the resistivity curves as $\ln(\rho/T) \sim 1/T$ because it is commonly accepted that the transport mechanism of the insulating regime of $La_{1-x}Sr_xMnO_3$ is the magnetic polaron transport.[20–22] Figure 5(b) shows that in the range of $T > T_C$ the curves are compatible with linearity quite well. And the activation energy obtained from fitting is 82 meV ($x=0$), 84 meV ($x=0.04$), and 111 meV ($x=0.16$). For the samples with $x=0.18$ and 0.20, we plot the $\ln(\rho/T) \sim 1/T$ curves as well as the variable-range hopping relation $\ln \rho \sim T^{1/4}$ in Fig. 5(c) and Fig. 5(d) to compare. For the sample with $x=0.18$, Fig. 5(c) indicates that the two relations can fit the curve well in different temperature range. For the sample with $x=0.20$, Fig. 5(d) gives that the $\ln(\rho/T) \sim 1/T$ curve apparently deviates from linearity while the $\ln \rho \sim T^{1/4}$ curve correspond with linearity quite well. All the fitting results suggest that the transport mechanism transits from the polaron transport to variable-range hopping with the increase of Cu ions. Obviously, with the adding of Cu, the e_g electrons of Mn^{3+} ions become localized, which increases the activation energy. When the content of Cu reaches 0.18, the e_g electrons of Mn^{3+} ions are more localized and the activation energy becomes very large, so the e_g electrons cannot hop in low temperature which causes that the polaron transport does not dominate. At the same time, the DE interaction cannot occur in the system. So the electron spins form a random magnetic structure instead of FM alignment. Hence, the low temperature resistivity can be fitted well by the Mott variable-range hopping relation.[23] With the continuous increasing of Cu, more severe magnetic disorder forms in the sample, which destroys the environment needed by the formation of polarons. Hence, the transport process is dominant by variable-range hopping.

From the resistivity versus temperature curves, it can be found in Fig. 4 that the interfacial tunneling really exists. In $0 \leqslant x \leqslant 0.12$ the curves have two peaks which locate at T_{P1} and T_{P2}, respectively ($T_{P1} \geqslant T_{P2}$). Here the T_{P1} is the temperature of metalinsulator transition caused by PM-FM phase transition. The peak at T_{P1} is a sign that the polarons delocalize to naked carriers and the electrical conduction changes from polaron hopping to free carriers itinerating in FM environment. We list T_{P1}, T_{P2}, T_C and T_C^{onset} into Table I to compare. It can be seen that for the samples with $x \leqslant 0.06$, T_{P1} consists with T_C^{onset} and for the samples with $x=0.1$ and 0.12, T_{P1} consists with T_C. It is reasonable because with the increase of Cu content, PM-FM phase transition is broadened and the FM amplitude is weakened. So only when temperature is lower than T_C^{onset} and close to T_C, can the naked carriers delocalized from polarons increase to a certain amount and the metallic property appears. Therefore the T_{P1} of the samples with $x=0.1$ and 0.12 is close to T_C. The peaks at T_{P2} are believed to reflect the spin-dependent interfacial tunneling due to the difference in magnetic order be-

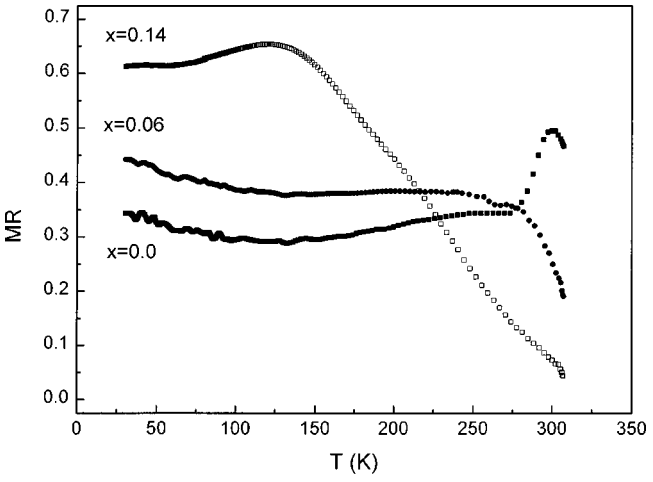

FIG. 7. The magnetoresistance curves of $La_{0.825}Sr_{0.175}Mn_{1-x}Cu_xO_3$. The applied magnetic field is 5 T.

tween surface and core.[24] In heavily doped range, the grain sizes of the samples are relatively small (seen from Fig. 6, the scanning electronic microscope photo). So the grain surface expands with the increase of x and the conductive channels gradually reduces. Hence, the contribution to the resistance of the interfacial tunneling becomes larger than that of the grain core and the height of the peaks at T_{P2} exceeds that of the peaks at T_{P1} gradually. In the range of $0.14 \leqslant x \leqslant 0.16$, the peak which reflects the magnetic transition is overwhelmed by that of the interfacial tunneling. So there is only one peak on the curve.

We measured the resistivity at applied magnetic fields of $x=0$, $x=0.06$ and $x=0.14$ samples. The magnetoresistance (MR) as a function of temperature is plotted in Fig. 7. Here the MR is defined as $\Delta\rho/\rho_0=(\rho_0-\rho_H)/\rho_0$, where ρ_0 is the resistivity at zero field and ρ_H is the resistivity at an applied magnetic field of 5 T. These samples all have pretty large negative magnetoresistance. And on the MR curves, there are corresponding peaks at the insulator-metal transition temperatures. The MR at T_{P2} can be attributed to the ionic spins in the surface being aligned by external field, which decreases the barrier height of the intergrain.[24] With the increase of x, the MR at T_{P2} increases because of the surface expansion.

IV. CONCLUSION

In summary, we have studied the effect of dilution of Mn by Cu on the electrical and magnetic properties of the CMR system $La_{0.825}Sr_{0.175}MnO_3$. The existence of Cu^{2+} weakens the long range ferromagnetic order in the $La_{0.825}Sr_{0.175}MnO_3$ and changes the transport mechanism of insulator phase from polaron transport to variable-range hopping. The double peak on $\rho \sim T$ curves indicates that the spin-dependent tunneling and intrinsic transport properties simultaneously exist in our samples.

ACKNOWLEDGMENTS

The authors would like to thank Dr. Yunhua Xu and Professor Fanqing Li for help in the experiments. This work was supported by the National Natural Science Foundation of China.

[1] C. W. Searle and S. T. Wang, Can. J. Phys. **47**, 2703 (1969).
[2] Ken-ichi Chahara, Toshiyuki Ohno, Masahiro Kasai, and Yuzoo Kozono, Appl. Phys. Lett. **63**, 1990 (1993).
[3] S. Jin, T. H. Tiefel, M. McCormack, R. A. Fastnacht, R. Ramesh, and L. H. Chen, Science **264**, 413 (1994).
[4] C. Zener, Phys. Rev. **82**, 403 (1951).
[5] W. Archibald, J.-S. Zhou, and J. B. Goodenough, Phys. Rev. B **53**, 14 445 (1995).
[6] A. J. Millis, Phys. Rev. B **53**, 8434 (1996).
[7] A. J. Millis, P. B. Littlewood, and B. J. Shraiman, Phys. Rev. Lett. **74**, 5144 (1995).
[8] A. Barnabé, A. Maignan, M. Hervieu, F. Damay, C. Martin, and B. Raveau, Appl. Phys. Lett. **71**, 3907 (1997).
[9] N. Gayathri, A. K. Raychaudhuri, S. K. Tiwary, R. Gundakaram, Anthony Arulraj, and C. N. R. Rao, Phys. Rev. B **56**, 1345 (1997).
[10] A. Tkachuk, K. Rogacki, D. E. Brown, B. Dabrowski, A. J. Fedro, C. W. Kimball, B. Pyles, X. Xiong, Daniel Rosenmann, and B. D. Dunlap, Phys. Rev. B **57**, 8509 (1998).
[11] Jian-Wang Cai, Cong Wang, Bao-Gen Shen, Jian-Gao Zhao, and Wen-Shan Zhan, Appl. Phys. Lett. **71**, 1727 (1997).
[12] J.-H. Park, S.-W. Cheong, and C. T. Chen, Phys. Rev. B **55**, 11 072 (1997).
[13] R. Von Helmolt, L. Haupt, K. Bärner, and U. Sondermann, Solid State Commun. **82**, 693 (1992).
[14] M. N. Iliev, H.-G. Lee, V. N. Popov, Y. Y. Sun, C. Thomsen, R. L. Meng, and C. W. Chu, Phys. Rev. B **57**, 2872 (1998).
[15] V. B. Podobedov, A. Weber, D. B. Romero, J. P. Rice, and H. D. Drew, Phys. Rev. B **58**, 43 (1998).
[16] J. B. Goodenough, A. Wold, R. J. Arnott, and N. Menyuk, Phys. Rev. **124**, 373 (1961).
[17] A. Shengelaya, Guo-Meng Zhao, H. Keller, and K. A. Muller, Phys. Rev. Lett. **77**, 5296 (1996).
[18] S. B. Oseroff, M. Torikachvili, J. Singley, S. Ali, S.-W. Cheong, and S. Schultz, Phys. Rev. B **53**, 6521 (1996).
[19] S. E. Lofland, P. K. P. Dahiroc, S. M. Bhagat, S. D. Tyagi, S. G. Karabashev, D. A. Shulyatev, A. A. Arsenov, and Y. Mukovskii, Phys. Lett. A **233**, 476 (1997).
[20] A. Millis, P. B. Littlewood, and B. I. Shraiman, Phys. Rev. Lett. **74**, 5144 (1995).
[21] H. Röder, J. Zang, and A. R. Bishop, Phys. Rev. Lett. **76**, 1356 (1996).
[22] G.-M. Zhao, K. Conder, H. Keller, and K. A. Müller, Nature (London) **381**, 676 (1996).
[23] N. F. Mott and E. A. Davis, *Electronic Processes in Noncrystalline Materials* (Clarendon Press, Oxford, 1979).
[24] Ning Zhang, Weiping Ding, Wei Zhong, Dingyu Xing, and Youwei Du, Phys. Rev. B **56**, 8138 (1997).